

# DESIGN AND SIMULATION OF MULTICHANNEL QCM DEVICES

Ahmad Anwar Zainuddin<sup>a</sup>, Mohd Asyraf Mohd Razib<sup>b\*</sup>, Amirul Taufiqurahman Ayob<sup>b</sup>, Nurain Sufi Sabreena Mohd Sukri<sup>c</sup>, Aliza Aini Md Ralib<sup>c</sup>

<sup>a</sup>Department of Computer Science, International Islamic University Malaysia, Selangor, Malaysia

<sup>b</sup>Department of Mechatronics Engineering, International Islamic University Malaysia, Kuala Lumpur, Malaysia

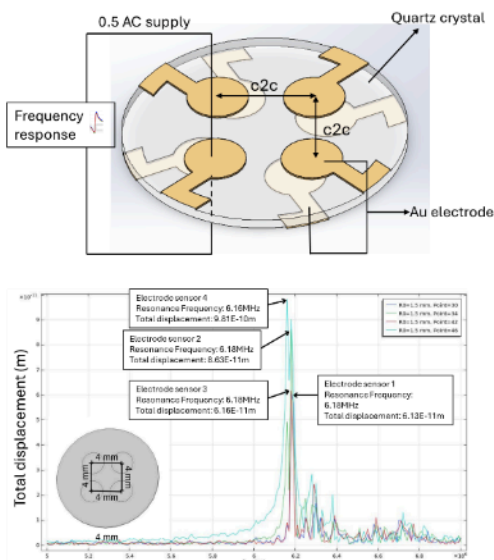
<sup>c</sup>Department of Electrical and Computer Engineering, International Islamic University Malaysia, Kuala Lumpur, Malaysia

## Article history

Received  
25 October 2024  
Received in revised form  
18 April 2025  
Accepted  
29 May 2025  
Published Online  
27 February 2026

\*Corresponding author  
asyrafr@iium.edu.my

## Graphical abstract



## Abstract

QCM (Quartz Crystal Microbalance) is a widely used biosensor in multiple industries and fields including medical, food safety and environmental health. However, its advances are predominantly focused on utilizing single channel on a QCM substrate. This limits the active area on QCM limited to the single channel and wastes the potential of the surface area of the substrate. The data received from a single channel QCM also lacks certainty where there is no other sensor that can verify or do cross-checking on its data real-time. The existing quartz thickness of 168 $\mu$ m does produce a high resonance frequency, however the QCM device is prone to break because of its extremely thin substrate, making it hard to handle. The aim of this study is to investigate, design and simulate the most significant parameters that contribute to the performance of multichannel QCM devices. The study examines the suitable quartz thickness and electrode sensor radius for single channel QCM, then proceeds to vary the c2c distance for multichannel QCM design. The study found that 1.5 mm is the optimal radius of electrode sensor for quartz thickness of 168  $\mu$ m single channel QCM with a resonance frequency of 6.17 MHz. 4 mm is the optimal c2c distance for 2-channel, 3-channel and 4-channel QCM. Future improvements on the multichannel QCM device should include introducing a sensing layer to detect certain compounds and using multiple channels on a single substrate to detect multiple compounds simultaneously.

**Keywords:** Multichannel Quartz Crystal Microbalance, Resonance Frequency, Interference Frequency, c2c distance and COMSOL Multiphysics

## Abstrak

QCM merupakan biosensor yang digunakan secara meluas dalam pelbagai bidang dan industri seperti perubatan, keselamatan makanan dan kesihatan alam sekitar. Walau bagaimanapun, kemajuannya lebih terhad kepada penggunaan satu saluran sensor pada substrat QCM. Ini mengehadkan luas permukaan kawasan aktif pada QCM hanya pada saluran sensor tunggal dan membazirkan potensi yang wujud pada lebih kawasan permukaan substrat. Bacaan yang diterima daripada satu saluran sensor QCM juga kurang kredibiliti di mana tiada sensor lain yang boleh mengesahkan atau melakukan pemeriksaan silang pada bacaan pada masa serentak. Ketebalan kuarza yang sedia ada pada 168  $\mu$ m memang menghasilkan

frekuensi resonans yang tinggi, namun QCM terlalu rapuh kerana substratnya sangat nipis, menyebabkan ia sukar untuk ditangani. Tujuan kajian ini adalah untuk menyiasat, merancang dan mensimulasikan ukuran-ukuran penting yang menyumbang kepada prestasi QCM dengan beberapa saluran sensor. Penyelidikan ini mengkaji ketebalan kuarza yang sesuai dan panjang jejari sensor elektrod untuk satu saluran sensor QCM, kemudian kajian diteruskan dengan mengubah jarak c2c untuk reka bentuk QCM dengan beberapa saluran sensor. Kajian ini mendapati bahawa 1.5 mm adalah panjang jejari optimum sensor elektrod untuk ketebalan kuarza 168  $\mu\text{m}$  QCM dengan satu saluran dengan frekuensi resonansi 6.17 MHz. 4 mm ialah jarak c2c yang optimal untuk 2 saluran, 3 saluran dan 4 saluran sensor QCM. Penambahbaikan yang boleh dilakukan pada peranti QCM dengan beberapa saluran sensor adalah dengan menggunakan lapisan pengesan untuk mengenal pasti sebatian tertentu dan menggunakan beberapa saluran pada substrat yang sama untuk mengesan beberapa sebatian berbeza pada masa yang sama.

**Kata kunci:** Multichannel Quartz Crystal Microbalance, Resonance Frequency, Interference Frequency, c2c distance and COMSOL Multiphysics

© 2026 Penerbit UTM Press. All rights reserved

## 1.0 INTRODUCTION

Biosensors can be used for various applications, such as detecting diseases in blood samples, monitoring water supply contaminants, and identifying foodborne pathogens like Salmonella [1], [2]. One of the most popular biosensor is Quartz Crystal Microbalance (QCM) that runs on the principle of acoustic waves and piezoelectricity [3][4]. QCM devices are broadly used for their high sensitivity, rapid response time and ability to provide real-time monitoring. Unfortunately, current research and fabrication efforts are predominantly focused on single-channel QCM. It does not fully utilize the available surface area of the QCM because the active sensing area becomes limited on the single channel's surface. Moreover, a single channel QCM is exposed to verification issues since readings from a single channel lacks reliability to confirm the accuracy of the data particularly in complex sensing environments.

Having a single channel on a QCM sensor limits the accuracy of the readings, making the data less reliable compared to setups with multiple channels [5], [6]. Besides, it restricts the ability to detect multiple chemical compounds on a single substrate, resulting in inefficient use of the available surface area and reduced overall efficiency. Therefore, the multichannel design in QCM provides great potential in maximizing the utilization of surface area, verifying data and enabling simultaneous sensing of multiple compounds that add versatility and broadens the application scope of QCM devices.

However, research on multichannel QCM sensors remains limited, particularly in finite element analysis (FEA). While FEA of single-channel QCM sensors has been extensively studied, focusing on resonance frequency shifts, sensitivity, and mechanical behavior under various conditions [7], [8], the understanding of multichannel QCM behavior through finite element

modeling is still underdeveloped. This gap hinders advancements in optimizing multichannel sensor designs. In this project, optimal design parameters will be investigated and simulated using COMSOL Multiphysics software, making this research a valuable contribution to the field of acoustic sensors and MEMS device design.

### 1.1 Acoustic Wave and Piezoelectricity

Piezoelectricity is the ability of certain materials to convert mechanical energy into electrical energy and vice versa [7]. When an electric potential is applied to a piezoelectric device, it generates kinetic energy as it vibrates at a consistent speed. This kinetic energy is then converted into electrical energy at the device's resonance frequency. Biosensor utilises two distinct types of piezoelectric sensors: the quartz crystal microbalance (QCM) and the surface acoustic wave (SAW) device. The QCM generates an acoustic wave that propagates within the volume of the sensor, whereas the SAW device generates a surface wave that propagates along the surface of the sensor.

Applying a voltage to the electrode will result in the conversion of the electrical signal into mechanical vibration in the form of an acoustic wave through the piezoelectric effect. The resonant frequency,  $f_r$ , is the precise frequency at which an acoustic wave oscillates at a higher amplitude. The size of the piezoelectric material will affect the resonant frequency  $f_r$ . Equation (1) determines the relationship between velocity ( $v$ ) and the dimension in thickness ( $d$ ) of the piezoelectric material.

$$f_r = \frac{v}{2d} \quad (1)$$

## 1.2 Sensitivity of QCM

The primary significance of mass sensitivity in a QCM is its role in detecting and quantifying specific compounds within the surrounding environment. Huang *et al.* [8] and Pan *et al.* [9] introduce several factors affecting the mass sensitivity of a QCM including shape, diameter, thickness and material of the electrode as well as the operating frequency of the quartz crystal.

The fundamental principle underlying the operation of QCM is described by the Sauerbrey equation. The QCM surface's mass-frequency relationship is described. The equation is as stated in Equation (2):

$$\Delta m = \frac{2f_0^2}{A(\rho_q\mu_q)^{1/2}} * \Delta f = -C_{QCM} * \Delta f \quad (2)$$

where  $\Delta m$  is the change in mass,  $f_0$  is the fundamental frequency of QCM,  $A$  is the effective area of QCM,  $\rho_q$  is the density of the quartz crystal and  $\mu_q$  is the shear modulus of the quartz crystal,  $\Delta f$  is the frequency shift while  $C_{QCM}$  is the mass sensitivity constant.

## 1.3 Interference Frequency

Previous studies have identified many methods to minimize the occurrence of frequency interference on a multichannel QCM. Shen *et al.* [10] asserts that the acoustic coupling between adjacent QCMs must be sufficiently minimal to ensure that the performance of each individual sensor is not influenced by the others. Two viable approaches involve enhancing the disparity in resonance frequency between the electroded and unelectroded segments of the plate, as well as modifying the respective dimensions of the electrodes. For MQCM with identical electrode size, higher interference effects are seen, necessitating a larger separation to mitigate frequency interference [11]. The disparity between the two resonant frequencies diminishes fast as the separation increases. When the distance between the two objects is sufficiently long, the two frequencies at which resonance occurs become very similar and approach the resonance frequency,  $\omega_0$ , of a single QCM with the same size of electrodes.

## 2.0 METHODOLOGY

### 2.1 Design Concept

#### 2.1.1 Substrate Material

The substrate material used to design a QCM is typically Quartz ( $\text{SiO}_2$ ), relevant to its name Quartz Crystal Microbalance. Quartz is used for its piezoelectricity characteristics which transforms mechanical energy from vibrations into electrical energy that produces frequency. An AT-cut quartz crystal typically used in a QCM has an acoustic wave of approximately  $3340 \text{ ms}^{-1}$  [12].

#### 2.1.2 Interdigital Transducer (IDT) Material

IDT material influences the mass sensitivity of the QCM. To enhance the functionality of QCM, gold is chosen as the IDT material for the electrode sensors as it has been proven that gold has 1.1 times higher mass sensitivity than silver [13].

#### 2.1.3 Thickness of the QCM

The primary emphasis in establishing the parameters of the QCM should be on its sensitivity [14]. In order to increase sensitivity, it is necessary for the quartz to be as thin as possible. Since  $168 \mu\text{m}$  is the lowest quartz thickness found from previous studies, the design parameter for the simulation of this project is to be simulated at a thickness of  $268 \mu\text{m}$ ,  $368 \mu\text{m}$ ,  $468 \mu\text{m}$ ,  $568 \mu\text{m}$ ,  $668 \mu\text{m}$  and  $768 \mu\text{m}$  to find the highest resonance frequency that is most compatible with other parameters.

#### 2.1.4 Diameter of the QCM

Previous works show that the biggest diameter of QCM that has been studied is  $14\text{mm}$ , thus it is selected in order to accommodate several electrode sensors on a single substrate, as the project seeks to replicate multichannel QCM [15]. The study aims to assess the boundaries of achieving the nearest proximity to the resonance frequency by placing several electrode sensors on a single substrate of quartz crystal.

#### 2.1.5 Thickness of the Electrode Sensor

The electrode sensor thickness influences the QCM's mass sensitivity and Q-factor [16]. A greater mass sensitivity value and Q-factor value are more favorable, and it has been proven that the electrode sensor with a higher thickness value will provide both higher mass sensitivity and Q-factor [17], [18]. The thickness of the electrode sensor is chosen as  $2000 \text{ \AA}$  or  $200 \text{ nm}$  since it is the highest thickness value of the electrode sensor that has been reviewed.

#### 2.1.6 Radius of the Electrode Sensor

The device's sensitivity is also dependent upon the electrode sensor's diameter. The mass sensitivity of the QCM is affected by the Gaussian distribution. This means that the mass sensitivity increases as the measurement comes closer to the center of the electrode which concludes that the radius must be small in order to obtain higher sensitivity. Previous studies have identified a  $2 \text{ mm}$  radius as the most optimal [19]. In this project, we will simulate various radii, including  $0.5 \text{ mm}$ ,  $1.0 \text{ mm}$ ,  $1.5 \text{ mm}$ ,  $2.0 \text{ mm}$ , and  $2.5 \text{ mm}$ , to identify which radius produces the highest mass sensitivity.

2.1.7 Number of Channels

The objective of this project is to simulate a multichannel QCM device. The simulation will involve 2, 3 and 4 channels, each featuring various center-to-center distances. The goal is to determine which pairing of number of channels and distance that can reach a resonance frequency, while minimizing any frequency interference.

2.1.8 Proposed Structure

Table 1 displays the summary of specifications and suggested design to be simulated in the project.

Table 1 Design parameter of multichannel QCM device

| Description               | Expression                                     |
|---------------------------|--|
| Substrate material        | Quartz   |
| Acoustic wave velocity    | 3340 ms <sup>-1</sup>                          |
| Substrate thickness       | 268 μm, 368 μm, 468 μm, 568 μm, 668 μm, 768 μm |
| Substrate diameter        | 14 mm  |
| Electrode sensor material | Gold (Au) [20]                                 |

2.2 COMSOL Multiphysics

The behavior of a multichannel QCM sensor was simulated using finite element simulation. The objective of the simulation is to investigate the optimum dimension of electrode with respect to number of channels of the design by measuring natural frequency and total displacement. The device parameter of the design is shown in Table 1. 3D diagram of QCM sensor is shown in Figure 1. An AC signal of 0.5V was applied on the top working electrode, and the other electrode was grounded. For meshing, the domain can be divided into triangular or quadrilateral subdivisions. A free triangular node has been used in this design to create an uniform triangular

mesh in 2D domain. The element size is set to normal. Then, the simulation is run using COMSOL Multiphysics to determine the resonance frequency, output voltage and output power. The resonance frequency theory can be calculated using Equation (1).

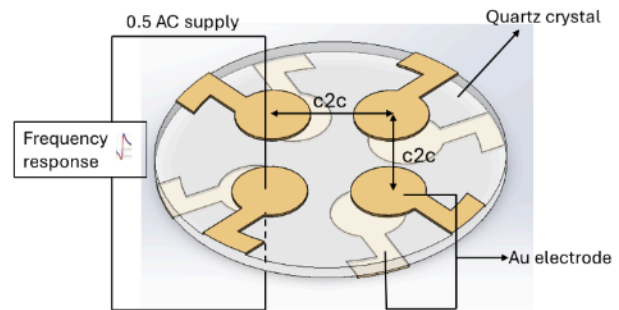


Figure 1 3D diagram of quartz crystal microbalance sensor

3.0 RESULTS AND DISCUSSION

The initial experiment was done by comparing the thickness of the quartz from the simulation that generated the best peak value on the graph plotted on COMSOL Multiphysics software. Subsequently, the electrode sensor radius most appropriate for the final chosen thickness of the quartz was determined by the maximum total displacement recorded during the simulation.

After choosing the best quartz thickness and the radius of the electrode sensor, the simulation is completed by the addition of the numbers of channels as well as varying centre to centre (c2c) distance in order to find out which combination will yield the least interference frequency while at the same time obtaining resonance frequency close to the resonance frequency obtained in the process of choosing the best value of quartz thickness.

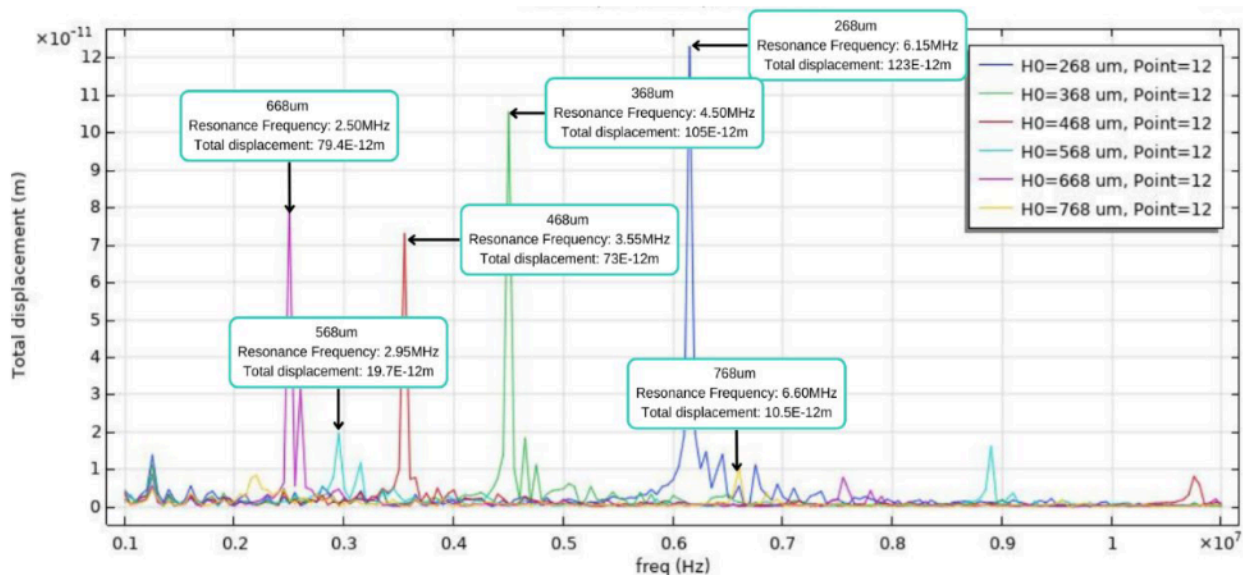


Figure 2 Graph plotted for varying quartz thickness simulation by COMSOL Multiphysics software

**3.1 Optimal Thickness of Quartz Based on Resonance Frequency**

The experiment was started by simulating thickness of quartz starting from 268 μm, 368 μm, 468 μm, 568 μm, 668 μm up to 768 μm. Quartz thickness that can produce the highest peak in resonance frequency in the graph is fit to be chosen as the optimal quartz thickness for QCM. Based on the simulation results in Figure 2, 268 μm produces the highest resonance frequency, thus making 6.15 MHz as the benchmark for resonance frequency for the upcoming experiments. Though 768 μm recorded higher resonance frequency of 6.60 MHz, the peak produced was significantly smaller compared to the rest of the quartz thickness as displayed in Figure 2, thus it can be disregarded.

**3.2 Optimal Electrode Sensor Radius Based on Displacement Amplitude**

By using 268 μm as the quartz thickness in addition to the previously set parameters, the simulation was continued by varying the radius of a single electrode sensor. The measurement of radius starts from 0.5 mm to 2.5 mm with an increment of 0.5 mm for each design.

Figure 3 shows the graph plotted by COMSOL Multiphysics software on the simulated design where the highest displacement amplitude was produced by 1.5 mm radius of electrode sensor. Based on the simulation, the smaller the radius of electrode sensor, the higher the resonance frequency until it arrived at a cutoff frequency. The sensitivity of electrode sensors decreased once it reached the cutoff frequency.

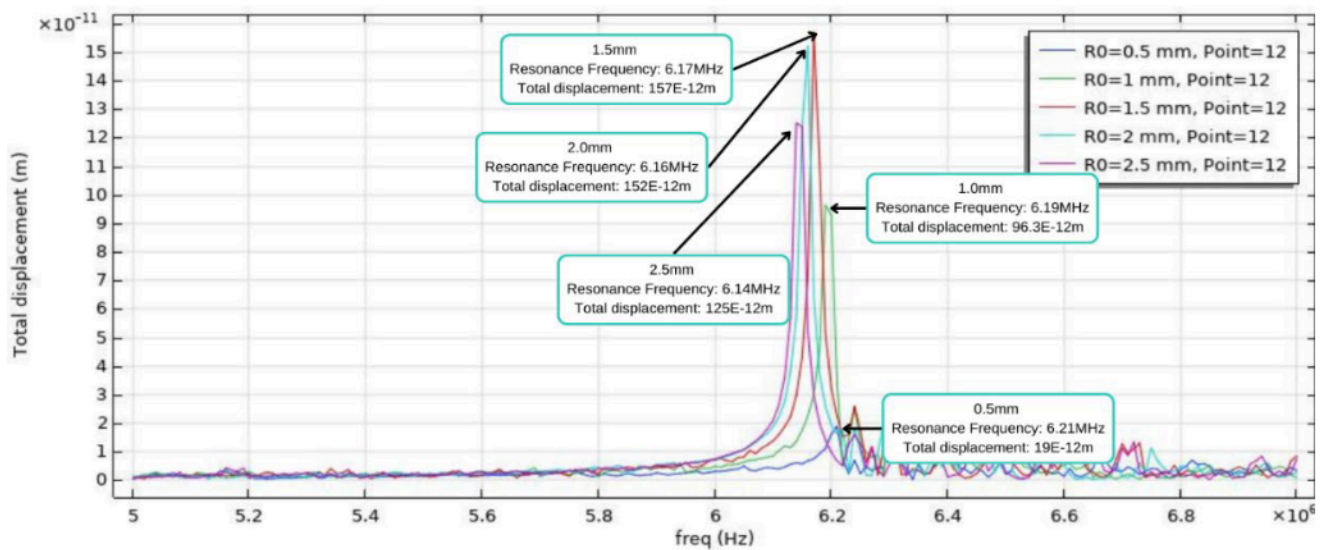


Figure 3 Graph plotted for varying radius of electrode sensor simulation by COMSOL Multiphysics software

The total displacement amplitude increases from 0.5 mm up to 1.5 mm and then the displacement decreases as the radius increases until 2.5 mm. This suggested that there is an optimal ratio between the quartz thickness and electrode sensor radius. The 268 μm thickness of quartz is compatible up to 1.5 mm only.

When compared between 0.5 mm, 1.0 mm and 1.5 mm of electrode sensor radius, it is found that 1.5 mm displayed the highest total displacement which suggested that 1.5 mm electrode sensor radius produces the most sensitive QCM for 268 μm quartz thickness. 6.17 MHz resonance frequency was noted as the benchmark for the next designs.

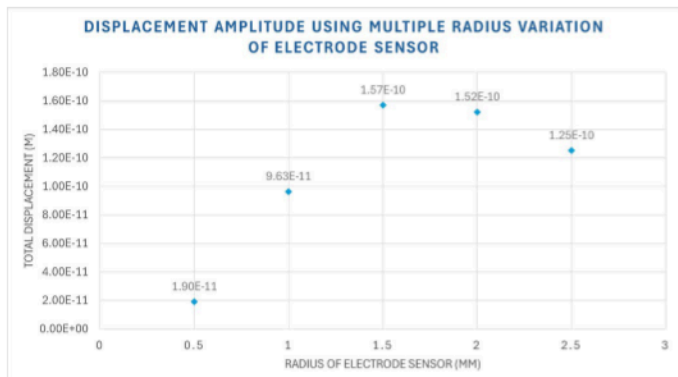


Figure 4 Comparison of displacement amplitude for variation of electrode sensor radius from 0.5 mm to 2.5 mm

**3.3 Interference in Multichannel QCM**

The QCM device were then designed using 2, 3 and 4 electrode sensors which indicates the 2, 3 and 4 channels of QCM. The aim in this experiment was to identify the optimal c2c distance for each number of channels by identifying the c2c distance that produces the least interference in frequency across all channels.

Graph plotted by the COMSOL Multiphysics software to illustrate the result produced line graphs of contrasting peak heights where some peak height might be evidently smaller than others. The distinct peak heights happens because the particular

electrode sensor becomes unstable since the electrode sensors were in close proximity to each other, and any electrode sensor may undergo this effect. This condition resulted in frequency interference in the electrode sensors' resonance frequency peak. The value of resonance frequency remains at around 6.17 MHz even though the peak was considerably smaller.

3.3.1 2-channel QCM

Using 268 μm quartz thickness and 1.5 mm electrode sensor radius, a 2-channel QCM was designed starting from 3 mm c2c distance where one point on the edge of each electrode sensors touched each other up until the maximum distance 10 mm where the electrode sensors were almost at the edges of the quartz.

High interference frequency was recognized where in Figure 5 for instance, at 9 mm c2c distance, a remarkable peak was less visible and a lot of noise were present instead around the peak. Table 2 concludes the findings of the simulations and Figure 6 displays the pattern and interference frequency between both electrode sensors.

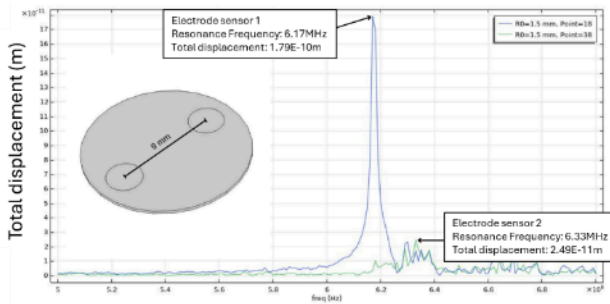


Figure 5 Simulation outcome for 2-channel QCM with 9mm c2c distance

Table 2 Resonance frequency for both channels of electrode sensor in 2-channel QCM design

| c2c distance (mm) | Sensor 1 Resonance Frequency (MHz) | Sensor 2 Resonance Frequency (MHz) |
|-------------------|------------------------------------|------------------------------------|
| 3                 | 6.16                               | 6.20                               |
| 4                 | 6.17                               | 6.18                               |
| 5                 | 6.17                               | 6.18                               |
| 6                 | 6.17                               | 6.18                               |
| 7                 | 6.17                               | 6.18                               |
| 8                 | 6.17                               | 6.33                               |
| 9                 | 6.17                               | 6.33                               |
| 10                | 6.17                               | 6.17                               |

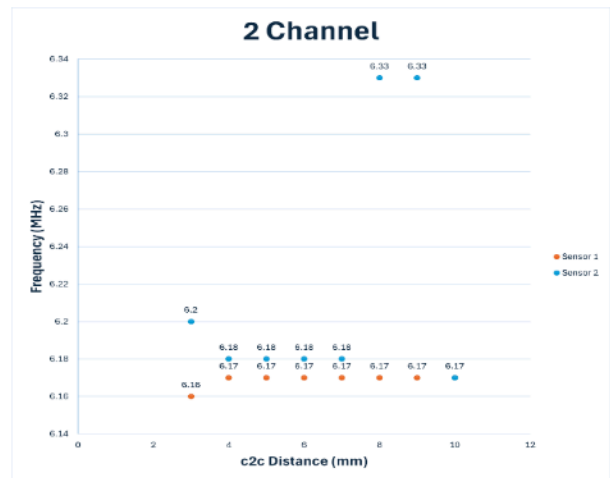


Figure 6 Summary of variations of simulated c2c distance for 2-channel QCMs

Simulations of 2-channel QCM at 3 mm, 8 mm, 9 mm were meaningless since they either produce high interference frequency and one of the electrode sensors' resonance frequencies deviated too far as can be seen in Table 2. As for 10 mm c2c distance, resonance frequency took place at the same time. All four designs were not to be considered as the optimal c2c distance for 2-channel QCM.

Design of 2-channel QCM with 4 mm c2c distance exhibited the best simulation results with resonance frequency close to the benchmark of 6.17 MHz as in Table 2 with a remarkable peak with minimal interference frequency as in Figure 7 as compared to the remaining three designs with c2c distance of 5 mm, 6 mm and 7 mm.

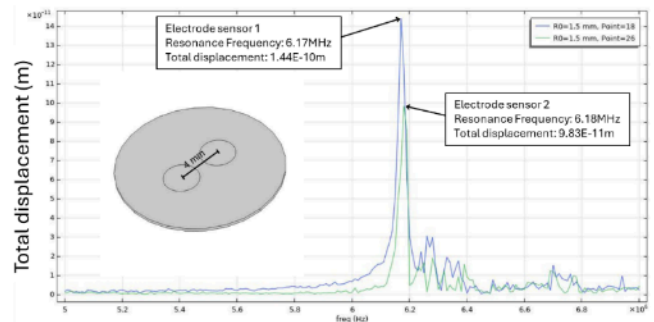


Figure 7 Simulation outcome for 2-channel QCM with 4mm c2c distance

3.3.2 3-channel QCM

Another channel was added on the quartz surface of the QCM design to facilitate 3-channel QCM design simulation. The design started from the closest c2c distance of 3mm, up to the maximum 8 mm of which the surface of the QCM can accommodate with an increment of 1mm for every succeeding design.

Figure 8 illustrated high frequency interference occurred in 3mm c2c distance for 3-channel QCM. A series of noise was present close to the highest peak which suggested that this design is not suitable to be considered as the optimal design. The same circumstances can be associated to 6mm, 7mm and 8mm designs. Table 3 concludes the findings of the simulations and Figure 9 displays the pattern and interference frequency between both electrode sensors.

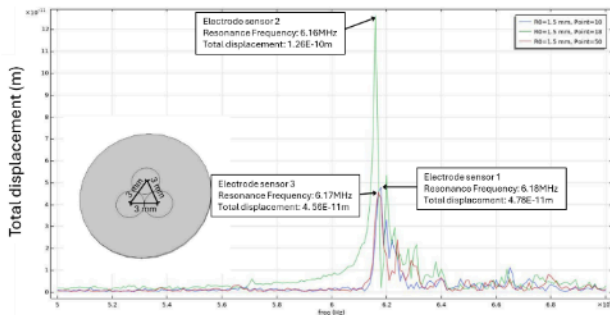


Figure 8 Simulation outcome for 3-channel QCM with 3mm c2c distance

Table 3 Resonance frequency for all channels of electrode sensor in 3-channel QCM design simulations

| c2c distance (mm) | Sensor 1 Resonance Frequency (MHz) | Sensor 2 Resonance Frequency (MHz) | Sensor 3 Resonance Frequency (MHz) |
|-------------------|------------------------------------|------------------------------------|------------------------------------|
| 3                 | 6.18                               | 6.16                               | 6.17                               |
| 4                 | 6.18                               | 6.18                               | 6.17                               |
| 5                 | 6.18                               | 6.17                               | 6.18                               |
| 6                 | 6.23                               | 6.17                               | 6.23                               |
| 7                 | 6.24                               | 6.17                               | 6.24                               |
| 8                 | 6.26                               | 6.17                               | 6.26                               |

Results from simulation of 6mm, 7mm and 8mm c2c distance for 3 channel QCMs in Table 3 suggested that these designs can be discarded since resonance frequency of two of the electrode sensors diverged from the resonance frequency 6.17 MHz that had been set as the point of reference. According to summary in Figure 9, QCM design with 4 mm and 5 mm c2c distance displayed satisfactory result where both can be considered for the optimal c2c distance for 3-channel QCM since both produces resonance frequency close to the point of reference frequency of 6.17 MHz and generated a plotted graph with less noise and interference frequency.

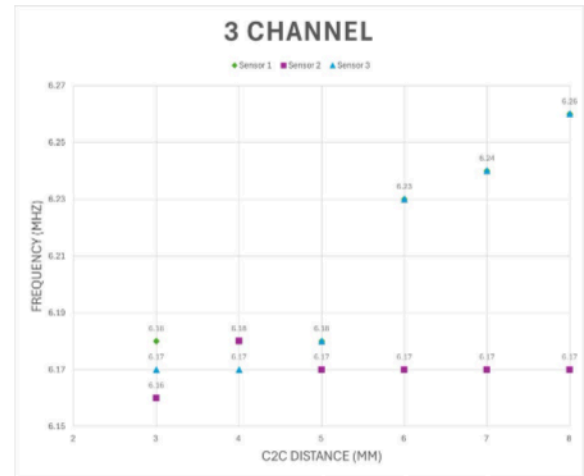


Figure 9 Summary of variations of simulated c2c distance for 3-channel QCMs

4 mm c2c distance was concluded as the optimal design for 3-channel QCM because all three electrode sensors exhibited higher peaks in Figure 10 which suggested the total displacement is higher, hence it meant that these electrode sensors had higher sensitivity as compared to 5 mm c2c distance where in Figure 11, two of the electrode sensors showed smaller peak value for the total displacement.

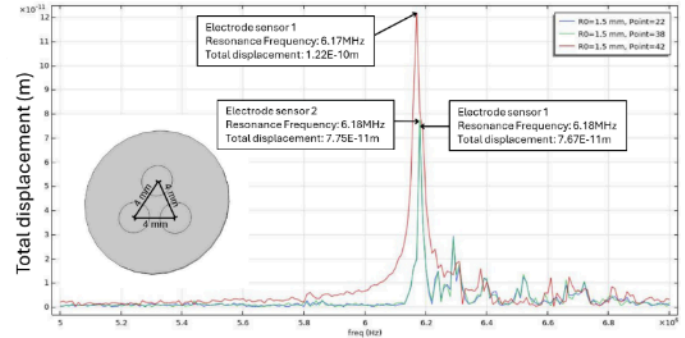


Figure 10 Simulation outcome for 3-channel QCM with 4 mm c2c distance

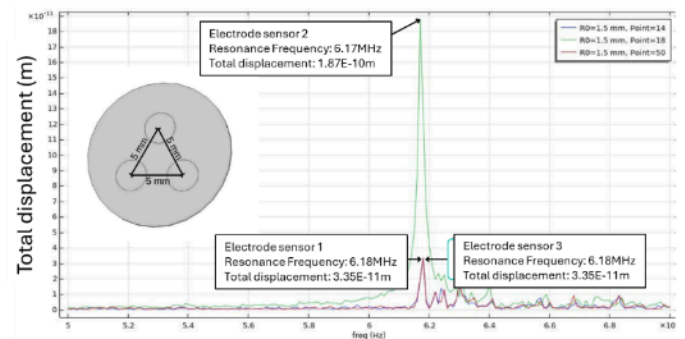


Figure 11 Simulation outcome for 3-channel QCM with 5 mm c2c distance

3.3.3 4-channel QCM

The 4-channel QCM designs were simulated with electrode distances ranging from a minimum of 3 mm (center-to-center) to a maximum of 7 mm, which was the farthest the electrode sensors could be positioned apart before losing contact with the quartz surface. The 4-channel QCM designs with electrode distances of 3 mm, 6 mm, and 7 mm (c2c), as shown in Figures 12, 13, and 14, respectively, were simulated to achieve resonance frequencies near the benchmark of 6.17 MHz. However, all three configurations exhibited significant noise in their frequency response graphs, rendering them unsuitable for practical use. All three designs clearly demonstrated why they are unsuitable for a 4-channel QCM configuration.

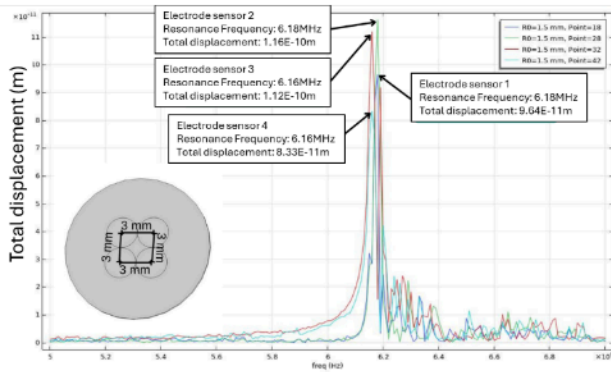


Figure 12 Simulation outcome for 4-channel QCM with 3 mm c2c distance

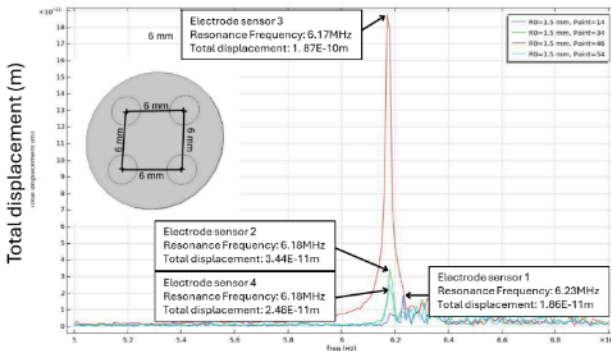


Figure 13 Simulation outcome for 4-channel QCM with 6 mm c2c distance

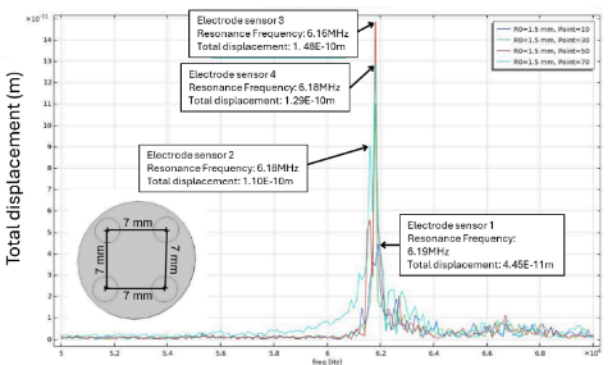


Figure 14 Simulation outcome for 4-channel QCM with 7 mm c2c distance

Table 4 summarizes the simulation results, and Figure 15 shows the pattern and interference frequency between both electrode sensors.

Table 4 Resonance frequency for all channels of electrode sensor in 4-channel QCM design simulations

| c2c distance (mm) | Sensor 1 Resonance Frequency (MHz) | Sensor 2 Resonance Frequency (MHz) | Sensor 3 Resonance Frequency (MHz) | Sensor 4 Resonance Frequency (MHz) |
|-------------------|------------------------------------|------------------------------------|------------------------------------|------------------------------------|
| 3                 | 6.18                               | 6.18                               | 6.16                               | 6.16                               |
| 4                 | 6.18                               | 6.18                               | 6.18                               | 6.16                               |
| 5                 | 6.19                               | 6.18                               | 6.17                               | 6.18                               |
| 6                 | 6.23                               | 6.18                               | 6.17                               | 6.18                               |
| 7                 | 6.19                               | 6.18                               | 6.18                               | 6.18                               |

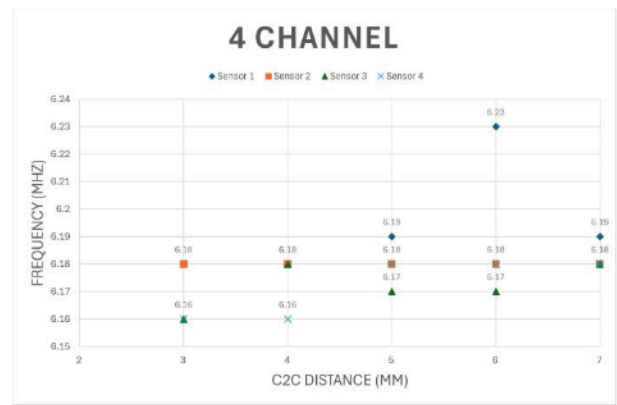
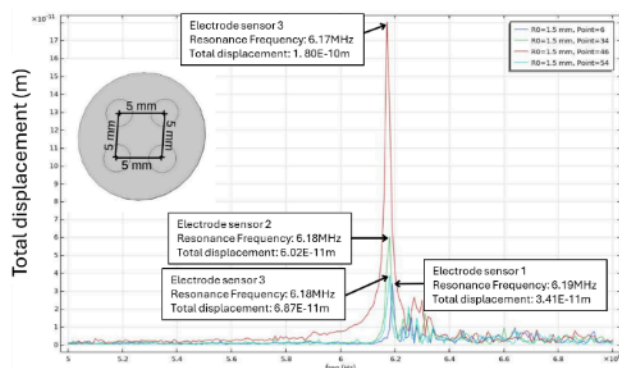
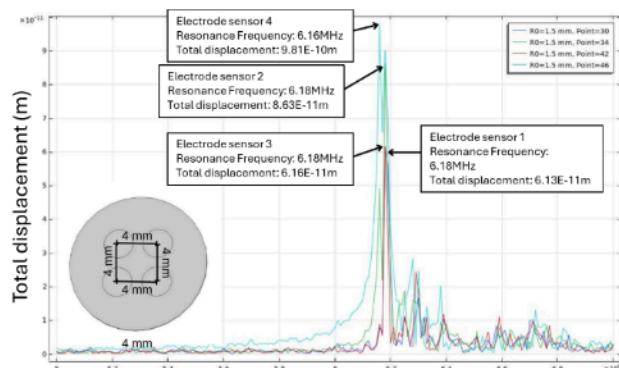


Figure 15 Summary of variations of simulated c2c distance for 3-channel QCMs

As shown in Figure 14, the QCM design with a 6 mm center-to-center electrode distance can be dismissed, as one of the electrode sensors experienced high-frequency interference, producing a resonance frequency of 6.23 MHz. To compare the QCM designs with 4 mm and 5 mm c2c electrode distances, both exhibiting resonance frequencies near the reference value of 6.17 MHz with minimal interference, the peak height was considered as an additional criterion. Three electrode sensors in Figure 16 produced distinctly smaller peaks than the other electrode sensor in 5 mm c2c distance for 4-channel QCM design while electrode sensors in Figure 17 produced smaller difference in peak heights for 4 mm c2c distance. Therefore, 4 mm c2c distance was selected as the best design for 4-channel QCM. Table 5 presents a comparative summary of previous studies related to QCM-based sensor systems and highlights the key differences and research gaps addressed in the current study.



**Figure 16** Simulation outcome for 4-channel QCM with 5 mm c2c distance



**Figure 17** Simulation outcome for 4-channel QCM with 4 mm c2c distance

**Table 5** Comparison of previous works to the current research study

| Author                 | Year | Title   | Findings   |
|------------------------|------|---|--|
| Aliza Aini et al. [21] | 2019 | Investigation on the mass sensitivity of quartz crystal microbalance gas sensor using finite element simulation | Finite element analysis for single channel QCM sensor only.  |
| Amer et al. [22]       | 2019 | Multichannel QCM-Based System for Continuous Monitoring of Bacterial Biofilm Growth                             | Multichannel system for continuous, online monitoring of bacterial biofilm formation. However, only single design is used throughout the experiment.             |
| Bourennane et al. [23] | 2023 | Accurate Multi-Channel QCM Sensor Measurement Enabled by FPGA-Based Embedded System Using GPS                   | Real-time frequency measurement system for high-precision, multi-channel quartz crystal microbalance (QCM) sensors using a field programmable gate array (FPGA). |
| Yoshiminen et al. [24] | 2023 | Pocketable Biosensor Based on Quartz-Crystal Microbalance and Its Application to DNA Detection                  | IC card-sized quartz-crystal microbalance (QCM) device for label-free DNA detection.   |
| Anwar et al.           | 2025 | This study  | Finite element analysis for multichannel QCM sensor  |

This study represents a pioneering effort in the finite element analysis (FEA) of multichannel quartz crystal microbalance (QCM) sensors. While previous research, such as Aliza Aini et al.'s 2019 work, focused on single-channel QCM sensors using FEA. This study extends the methodology to multichannel configurations. Although multichannel QCM systems have been designed and tested, none have employed a similar FEA approach to analyze their

performance. This novel application of FEA to multichannel QCM sensors addresses the complexities of inter-channel interactions and resonance behaviors, thereby contributing significantly to the advancement of sensor design and optimization.

## 4.0 CONCLUSION

This study designed, simulated, and optimized a multichannel quartz crystal microbalance (QCM) to enhance the efficiency and fully realize the potential of single-channel QCM systems. The optimal quartz thickness within the range of 268  $\mu\text{m}$  to 768  $\mu\text{m}$  is 268  $\mu\text{m}$ , yielding a resonance frequency of 6.15 MHz. The electrode sensor radius that has the highest mass sensitivity for 268  $\mu\text{m}$  quartz thickness is 1.5 mm which produces a resonance frequency of 6.17 MHz. The optimal c2c distance that produces higher resonance frequency with minimal frequency interference is 4 mm for all 2-channel, 3-channel and 4-channel QCM. Single channel QCM was improved to a multichannel QCM to facilitate sensing multiple compounds simultaneously. This study successfully identifies the optimal design for multichannel QCM systems. Future improvement should be done to apply multichannel QCM in sensing multiple products simultaneously in a real-life application.

## Acknowledgement

The author would like to acknowledge financial assistance from Research Management Centre, International Islamic University, Malaysia (RMC-IIUM). This study was also supported by the Ministry of Higher Education (MOHE) Fundamental Research Grant Scheme FRGS21-248-0857.

## Conflicts of Interest

The authors declare that there is no conflict of interest regarding the publication of this paper.

## References

- [1] S. M., and S. Gandhi. 2022. Recent Advances in Electrochemical Biosensors for the Detection of Salmonellosis: Current Prospective and Challenges. *Biosensors*. 12(365). <https://doi.org/10.3390/foods12142795>.
- [2] Castillo-Henríguez, L., M. Brenes-Acuña, A. Castro-Rojas, R. Cordero-Salmerón, M. Lopretti-Correa, and J. R. Vega-Baudrit. 2020. Biosensors for the Detection of Bacterial and Viral Clinical Pathogens. *Sensors*. 20(23): 1–26. <https://doi.org/10.3390/s20236926>.
- [3] Alanazi, N., M. Almutairi, and A. N. Alodhayb. 2023. A Review of Quartz Crystal Microbalance for Chemical and Biological Sensing Applications. Vol. 24, no. 1. Springer US. <https://doi.org/10.1007/s11220-023-00413-w>.
- [4] Orlando, J., T. Diaz, and A. F. Velásquez. 2024. QCM Biosensors for Pathogen Detection in Water and Food: Review of Published Literature. *Ingeniería Solidaria*. 20(2).
- [5] Tuantranont, A., A. Wisitsora-at, P. Sritongkham, and K. Jaruwongrunsee. 2011. Monolithic Multichannel Quartz Crystal Microbalance: A Review. *Analytica Chimica Acta*. 687(2): 114–128. <https://doi.org/10.1016/j.aca.2010.12.022>.
- [6] Amer, M. A., A. Turo, J. Salazar, L. Berlanga-Herrera, M. J. Garcia-Hernandez, and J. A. Chavez. 2020. Multichannel QCM-Based System for Continuous Monitoring of Bacterial Biofilm Growth. *IEEE Transactions on Instrumentation and Measurement*. 69(6): 2982–2995. <https://doi.org/10.1109/TIM.2019.2929280>.
- [7] Ralib, A. A. M., N. N. B. N. M. Zamri, A. H. F. Hazadi, R. A. Rahim, N. F. Za'Bah, and N. Saidin. 2019. Investigation on the Mass Sensitivity of Quartz Crystal Microbalance Gas Sensor Using Finite Element Simulation. *Bulletin of Electrical Engineering and Informatics*. 8(2): 460–469. <https://doi.org/10.11591/eei.v8i2.1521>.
- [8] Huang, X., Q. Chen, W. Pan, and Y. Yao. 2022. Advances in the Mass Sensitivity Distribution of Quartz Crystal Microbalances: A Review. *Sensors*. 22(14). <https://doi.org/10.3390/s22145112>.
- [9] Pan, W., X. Huang, and Q. Chen. 2020. Uniformization of Mass Sensitivity Distribution of Silver Electrode QCM. *IEEE Transactions on Ultrasonics, Ferroelectrics, and Frequency Control*. 67(9): 1953–1956. <https://doi.org/10.1109/TUFFC.2020.3008790>.
- [10] Shen, F., S. J. O'Shea, K. H. Lee, P. Lu, and T. Y. Ng. 2003. Frequency Interference between Two Mesa-Shaped Quartz Crystal Microbalances. *IEEE Transactions on Ultrasonics, Ferroelectrics, and Frequency Control*. 50(6): 668–675. <https://doi.org/10.1109/TUFFC.2003.1209554>.
- [11] Shen, Feng, and Pin Lu. 2004. Influence of Interchannel Spacing on the Dynamical Properties of Multichannel Quartz Crystal Microbalance. *IEEE Transactions on Ultrasonics, Ferroelectrics, and Frequency Control*. 51(2): 249–253. <https://doi.org/10.1109/TUFFC.2004.1320773>.
- [12] Rodahl, M., and B. Kasemo. 1996. Frequency and Dissipation-Factor Responses to Localized Liquid Deposits on a QCM Electrode. *Sensors and Actuators B: Chemical*. 37(1–2): 111–116. [https://doi.org/10.1016/S0925-4005\(97\)80077-9](https://doi.org/10.1016/S0925-4005(97)80077-9).
- [13] Huang, X., Q. Chen, W. Pan, and J. Hu. 2019. Assessing the Mass Sensitivity for Different Electrode Materials Commonly Used in Quartz Crystal Microbalances (QCMs). 1–7.
- [14] Songkhla, S. N., and T. Nakamoto. 2021. Overview of Quartz Crystal Microbalance Behavior Analysis and Measurement. *Chemosensors*. 9(12): 350. <https://doi.org/10.3390/chemosensors9120350>.
- [15] Milsom, A., S. Qi, A. Mishra, T. Berkemeier, Z. Zhang, and C. Pfrang. 2023. Technical Note: In Situ Measurements and Modelling of the Oxidation Kinetics in Films of a Cooking Aerosol Proxy Using a Quartz Crystal Microbalance with Dissipation Monitoring (QCM-D). *Atmospheric Chemistry and Physics*. 23(19): 10835–10843. <https://doi.org/10.5194/acp-23-10835-2023>.
- [16] Hu, J., X. Huang, and H. Lin. 2018. Study on QCM Mass Sensitivity for Different Electrode Structures. In *Proceedings of the 2018 IEEE International Conference on Applied Superconductivity and Electromagnetic Devices (ASEMD)*. 1–2. <https://doi.org/10.1109/ASEMD.2018.8558872>.
- [17] Wei, Z., J. Hu, Y. Li, and J. Chen. 2022. Effect of Electrode Thickness on Quality Factor of Ring Electrode QCM Sensor. *Sensors*. 22(14). <https://doi.org/10.3390/s22145159>.
- [18] Huang, X., Q. Chen, W. Pan, and J. Hu. 2021. The Effect of Electrode Thickness on Mass Sensitivity of QCM Cannot Be Ignored. *IEEE Transactions on Ultrasonics, Ferroelectrics, and Frequency Control*. 68(4): 1458–1461. <https://doi.org/10.1109/TUFFC.2020.3030636>.
- [19] Zainuddin, A. A., A. N. Nordin, A. F. Mohd Mansor, R. Ab Rahim, and W. C. Mak. 2020. Integrated Multichannel Electrochemical-Quartz Crystal Microbalance Sensors for Liquid Sensing. *IEEE Access*. 8: 3668–3676. <https://doi.org/10.1109/ACCESS.2019.2962324>.
- [20] Chen, Q., X. Huang, Y. Yao, and K. Mao. 2022. Analysis of the Effect of Electrode Materials on the Sensitivity of Quartz Crystal Microbalance. *Nanomaterials*. 12(6). <https://doi.org/10.3390/nano12060975>.
- [21] Ralib, A. A. M., N. N. B. N. M. Zamri, A. H. F. Hazadi, R. A. Rahim, N. F. Za'Bah, and N. Saidin. 2019. Investigation on the Mass Sensitivity of Quartz Crystal Microbalance Gas Sensor Using Finite Element Simulation. *Bulletin of Electrical*

- Engineering and Informatics*. 8(2): 460–469. <https://doi.org/10.11591/eei.v8i2.1521>.
- [22] Amer, M. A., A. Turo, J. Salazar, L. Berlanga-Herrera, M. J. Garcia-Hernandez, and J. A. Chavez. 2020. Multichannel QCM-Based System for Continuous Monitoring of Bacterial Biofilm Growth. *IEEE Transactions on Instrumentation and Measurement*. 69(6): 2982–2995. <https://doi.org/10.1109/TIM.2019.2929280>.
- [23] Bourenane, A., C. Tanougast, C. Diou, and J. Gorse. 2023. Accurate Multi-Channel QCM Sensor Measurement Enabled by FPGA-Based Embedded System Using GPS. *Electronics*. 12(12). <https://doi.org/10.3390/electronics12122666>.
- [24] Yoshimine, Hiroshi, Kai Sasaki, and Hiroyuki Furusawa. 2022. Pocketable Biosensor Based on Quartz-Crystal Microbalance and Its Application to DNA Detection. *Sensors*. 23(1): 281. <https://doi.org/10.3390/s23010281>.